Model Predictive Control of Underactuated Bipedal Robotic Walking

Matthew J. Powell, Eric A. Cousineau, and Aaron D. Ames

Abstract— **This paper addresses the problem of controlling underactuated bipedal walking robots in the presence of actuator torque saturation. The proposed method synthesizes elements of the Human-Inspired Control (HIC) approach for generating provably-stable walking controllers, rapidly exponentially stabilizing control Lyapunov functions (RES-CLFs) and standard model predictive control (MPC). Specifically, the proposed controller uses feedback linearization to construct a linear control system describing the dynamics of the walking outputs. The input to this linear system is designed to be the solution of a MPC-based Quadratic Program which minimizes the sum of the values of a RES-CLF–describing the walking control objectives–over a finite-time horizon. Future values of the torque constraints are mapped into the linear control system using the Hybrid Zero Dynamics property of HIC and subsequently incorporated in the Quadratic Program. The proposed method is implemented in a rigid-body dynamics simulation and initial experiments with the Durus robot.**

I. Introduction

Model-based control of bipedal robotic walking can be broadly classified into two groups, low-dimensional and high-dimensional model-based controllers. In the former, some approaches utilize models related to the dynamics of the robot's center of mass in the design of controllers which dictate the aggregate behavior of the robot. The most common low-dimensional models incorporated in robot walking controllers are the Linear Inverted Pendulum [10], [12], [19], [22], the Spring-Loaded Inverted Pendulum [8], and the full nonlinear center of mass dynamics [12]. An advantage shared by most low-dimensional walking controllers is that they can be implemented in real-time control systems. However, when formal hybrid stability of the walking controller is required, as determined through Poincare analysis [15], the full (high-dimensional) dynamics must be considered and thus, controller generation cannot generally be solved in real-time. These methods include direct trajectory optimization [18], Hybrid Zero Dynamics [9], and the method discussed in this paper, Human-Inspired Control [1], among others. Due to the complexity of the high-dimensional model, these optimization problems generally have to be solved apriori, or "offline", producing optimal control parameters that can then be implemented "online" through local nonlinear control. This paper presents an alternative, Model-Predictive Control, approach to the online implementation of walking gaits obtained apriori through the Human-Inspired Control framework.

Matthew J. Powell, Eric A. Cousineau, and Aaron D. Ames are with the Department of Mechanical Engineering, Texas A&M University, College Station, TX 77843. {mjpowell,eacousineau,aames}@tamu.edu

This research is supported by NASA grants NNX11AN06H and NNX12AQ68G, NSF grants CPS-1239085, CNS-0953823 and CNS-1136104, and the Texas Emerging Technology Fund.

The goal of the Human-Inspired Control approach is to produce exponentially stable periodic orbits–corresponding to stable walking–in a hybrid system model of the robot. This goal is realized by using constrained nonlinear optimization to produce parameterized functions of the robot's state, termed virtual constraints or *outputs*, whose corresponding zero dynamics surface is invariant through impact, i.e. foot strike. After solving the optimization offline, the walking gait is implemented online via nonlinear control, in the form of feedback linearization [20] or rapidly exponentially stabilizing control Lyapunov functions (RES-CLF) [2], to locally stabilize the control objectives and in doing so, stabilize the periodic orbit corresponding to walking.

The nonlinear optimization problem can include additional constraints, such as actuator torque limits; however, overly restrictive constraints can render the problem infeasible. Recent work [7] addresses torque constraints through an online controller that uses a Quadratic Program (QP) to solve for torques that achieve rapid exponential stability of a Lyapunov function describing the walking outputs while simultaneously satisfying actuator torque limits. However, in general, convergence constraints and torque limits may not always be feasible, so a relaxation factor is added to the QP to allow for violation of the CLF constraint. This produces a locally optimal solution but does not guarantee behavior of the controller over an extended period of time. As a step toward guaranteeing forward horizon behavior of the RES-CLF under torque saturation, the controller proposed in this paper uses Model Predictive Control: a control framework that reasons about future convergence under input saturation.

The main contribution of this paper is an online controller which combines elements of Human-Inspired Control for bipedal robotic walking [1], the RES-CLF QP [3], [2], [7] and standard Model Predictive Control (MPC) [5], [11], [14]. The present MPC setup is most similar to the approach of [13] in which linear MPC methods are applied to the linear input/output control system obtained through feedback linearization of a nonlinear process. In the present method, elements of [13] are explictly computed in the context of Human-Inspired Control. In particular, the linear input/output control system obtained through feedback linearization of the human-inspired outputs is converted into a discrete-time system and used to construct a linear MPC-based quadratic program which minimizes the sum of the values of the RES-CLF over an extended period of time. Torque constraints in the nonlinear robot dynamics are mapped into the linear MPC-based QP through a procedure that uses Hybrid Zero Dynamics to estimate the future states of the robot. The end result extends the (local) RES-CLF QP to an MPC problem.

II. Control of Robotic Walking

This section presents an overview of the continuous-time component of the Human-Inspired Control (HIC) approach for underactuated bipedal robotic walking [1]. The goal of HIC is to produce exponentially stable periodic orbits–corresponding to stable walking–in a hybrid system model of the robot. This goal is realized by producing walking control objectives, or *outputs*, whose corresponding zero dynamics surface is invariant through impact, i.e. foot strike. Nonlinear control, in the form of feedback linearization [20] or rapidly exponentially stabilizing control Lyapunov functions [2], is used to locally stabilize the control objectives and in doing so, stabilize the periodic orbit corresponding to walking. The following paragraphs briefly cover the construction of the continuous-time controller in the context of HIC.

A. Control System Model

Consider a model of an *underactuated* robot comprised of n rigid links and $m = n - 1$ actuated revolute joints. Let $\theta = (\theta_b, \theta_a) \in Q \subset \mathbb{R}^n$ denote a vector of body coordinates with $\theta_a \subset \mathbb{R}^m$ a vector of "actuated joint angles" and $\theta_b \in \mathbb{R}$ a passive joint angle. Given this choice of coordinates, the standard robot manipulator dynamics (see [17], [21]) can be expressed as

$$D(\theta)\ddot{\theta} + C(\theta, \dot{\theta})\dot{\theta} + G(\theta) = Bu, \tag{1}$$

with inertia matrix $D(\theta)$, Coriolis matrix $C(\theta, \dot{\theta})$, gravity vector $G(\theta)$, actuator torque vector $u \in \mathbb{R}^m$ and torque distribution matrix B. For more details on the specific model considered in this paper, see [4]. These dynamics can be used to express a general nonlinear control system for the robot:

$$\dot{x} = f(x) + g(x)u, \tag{2}$$

in which $x = (\theta, \dot{\theta})^T \in TQ$. In the Human-Inspired Control approach, the goal is to realize exponentially stable periodic orbits in a hybrid system representation of the robot; the details of which are given in [1]. In the context of this paper, it suffices to say that the hybrid system is comprised of the continuous-time dynamics (2) and a discrete update law describing the post-impact state, $x^+ = (\theta^+, \dot{\theta}^+)^T$, following an inelastic collision of the robot with the ground:

$$x^+ = \Delta(x), \quad \text{if } x \in \mathcal{S}, \tag{3}$$

where $\mathcal{S}$ is the guard and Δ is the reset map of the hybrid system. To this end, a parameterized feedback control, $u(x, \alpha)$ is designed through careful construction of control objectives, or *outputs*, as described in the following paragraph.

B. Human-Inspired Control Objectives

In the Human-Inspired Control framework, the goal of effecting walking on the robot is realizing by driving continuous functions of the robot's joint angles to corresponding desired values, whose form is motivated by observations of human walking data [1]. The process involves constructing outputs $y(\theta) \in \mathbb{R}^m$ whose zeros correspond to a periodic orbit in the hybrid system. Continuous-time controllers, are designed to produce u that exponentially stabilize $y(\theta) \to \mathbf{0}$.

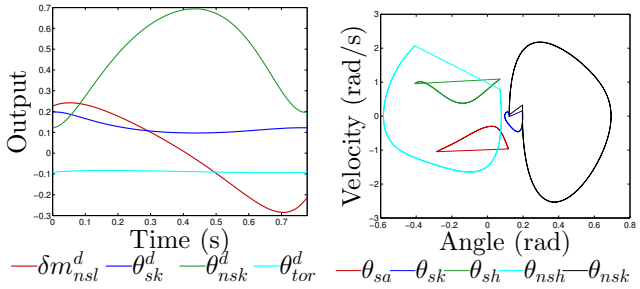

Fig. 1. Human-Inspired Walking Outputs (Left) and Periodic Orbits (Right). See [1], [4] for specific definitions of the robot joint angles and constructions of the walking outputs used in this paper.

The final form (see [4] for specific constructions used for the simulation and experiment examples in this paper) of these outputs is

$$y(\theta) = y^a(\theta) - y^d(\tau(\theta), \alpha), \tag{4}$$

where $y^a(\theta)$ is a vector of "actual" outputs and $y^d(\tau(\theta), \alpha)$ is a vector of "desired" outputs. The actual outputs can be nonlinear functions, but they most often take a linear form:

$$y^a(\theta) = H\theta, \tag{5}$$

where $H \in \mathbb{R}^{m \times n}$ has full (row) rank. The desired behaviors are encoded by the solution of an underdamped second order system:

$$y_{cwf}(t, \alpha) = e^{-\alpha_4 t}\left(\alpha_1 \cos(\alpha_2 t) + \alpha_3 \sin(\alpha_2 t)\right) + \alpha_5. \tag{6}$$

This function is made state-based through the substitution $t \to \tau(\theta)$, with $\tau(\theta)$ given by

$$\tau(\theta) = \frac{p_{hip}(\theta) - p_{hip}(\theta^+)}{v_d}, \tag{7}$$

and where $p_{hip}(\theta) := c\theta$, $c \in \mathbb{R}^{1 \times n}$, is the linearized forward position of the hip, and v_d is the walking speed of the robot. This particular *parameterization of time* is based on the observation that the forward position of the hip during walking evolves nearly linearly with respect to time. Substituting (7) into (6), the final form of the desired outputs, as shown in (4), becomes:

$$y^d(\tau(\theta), \alpha) = [y_{cwf}(\tau(\theta), \alpha^i)]_{i \in O}, \tag{8}$$

in which O is an indexing set used to match desired outputs with corresponding actual values. Associated with the parameters α is a zero dynamics surface:

$$\mathbf{Z}_\alpha = \{(\theta, \dot{\theta}) \in TQ : y(\theta) = \mathbf{0}, L_f y(\theta, \dot{\theta}) = \mathbf{0}\}, \tag{9}$$

on which the robot's actual behavior is identical to the prescribed desired behavior. In the Human-Inspired Control method, an optimization problem is solved to obtain parameters α^* that satisfy hybrid invariance of $\mathbf{Z}_\alpha$:

$$\Delta(\mathcal{S} \cap \mathbf{Z}_\alpha) \subset \mathbf{Z}_\alpha. \tag{10}$$

Theorem 3 of [1] gives conditions on α which, when satisfied in conjunction with (10), result in the existence of an exponentially stable periodic orbit (a stable walking gait) in a full-state hybrid system representation of the robot.

C. Local Nonlinear Control

This section describes nonlinear control methods which can be employed to exponentially stabilize the human-inspired walking outputs (4) within the robot control system (2). In particular, feedback linearization [20] can be used to achieve an arbitrary convergence rate when torque bounds are not considered. However, in the control of robotic locomotion, torque bounds cannot generally be neglected and thus a more sophisticated approach, like the one described in [2], [7], is required.

Input/Output (Feedback) Linearization. As the human-inspired outputs, $y(\theta)$, have vector relative degree two in the robot control system (2), the input/output linearization control law for these outputs is

$$u = A^{-1}(-L_f + \mu), \tag{11}$$

where $A := L_g L_f y(\theta)$ and $L_f := L_f^2 y(\theta, \dot{\theta})$ are Lie derivatives along the vector fields $f(x)$ and $g(x)$ and the dependence on $(\theta, \dot{\theta})$ has been suppressed for brevity. Here the decoupling matrix A is assumed to be invertible and can be made so through proper construction of control outputs $y(\theta)$. Applying (11) to (2) results in $\ddot{y} = \mu$. In the absence of torque constraints, a common choice of μ places the closed-loop poles of the output dynamics at $-1/\varepsilon$,

$$\mu = -\frac{2}{\varepsilon}\dot{y} - \frac{1}{\varepsilon^2}y, \tag{12}$$

where $0 < \varepsilon < 1$ determines the output convergence rate. When torque constraints cannot be neglected, as is often the case in robot locomotion, a more sophisticated method of selecting μ is required.

Control Lyapunov Functions. The rapidly exponentially stabilizing control Lyapunov Function (RES-CLF) framework presented in [2] provides a method of simultaneously satisfying torque constraints and achieving exponential stability. Assuming the preliminary feedback (11) has been applied, and defining the "output" coordinates $\eta := (y, \dot{y})^T$, results in the following linear system:

$$\dot{\eta} = \underbrace{\begin{bmatrix} 0 & 1 \\ 0 & 0 \end{bmatrix}}_{F} \eta + \underbrace{\begin{bmatrix} 0 \\ 1 \end{bmatrix}}_{G} \mu. \tag{13}$$

The method of [2] can be employed to construct a RES-CLF for the system (13) of the form, $V_\varepsilon(\eta) = \eta^T P_\varepsilon \eta$,

$$V_\varepsilon(\eta) = \eta^T \underbrace{I_\varepsilon P I_\varepsilon}_{P_\varepsilon} \eta, \quad I_\varepsilon := \operatorname{diag}\left(\frac{1}{\varepsilon} I, I\right), \tag{14}$$

where I is the identity matrix and $P = P^T > 0$ solves the continuous time algebraic Riccati equations (CARE)

$$F^T P + PF - PGG^T P + Q = 0 \tag{15}$$

for $Q = Q^T > 0$. The time-derivative of (14) is given by

$$\dot{V}_\varepsilon(\eta) = L_F V_\varepsilon(\eta) + L_G V_\varepsilon(\eta)\mu, \tag{16}$$

where the Lie derivatives of $V_\varepsilon(\eta)$ along the vector fields F and G are

$$L_F V_\varepsilon(\eta) = \eta^T (F^T P_\varepsilon + P_\varepsilon F)\eta, \tag{17}$$

$$L_G V_\varepsilon(\eta) = 2\eta^T P_\varepsilon G. \tag{18}$$

To achieve rapid exponential stability, and thus meet the requirements of a RES-CLF, the following inequality on $\dot{V}_\varepsilon$ must be satisfied

$$L_F V_\varepsilon(\eta) + L_G V_\varepsilon(\eta)\mu + \frac{\gamma}{\varepsilon} V_\varepsilon(\eta) \leq 0 \tag{19}$$

with $\gamma = \lambda_{\min}(Q)/\lambda_{\max}(P)$. In [2], it is shown that by applying a RES-CLF to the continuous-time robot control system (2), the corresponding periodic orbit (walking gait) is exponentially stabilized. The following paragraph describes an existing method for implementing a RES-CLF controller.

RES-CLF Quadratic Program. In practice, determining a μ that satisfies the RES-CLF constraint (in an optimal manner) can be achieved through the solution of a quadratic program (QP) [2]. Indeed, the structure of a QP facilitates inclusion of *any* affine constraint on μ, including actuator torque limits:

$$u = A^{-1}(-L_f + \mu) \leq u_{\max}, \tag{20}$$

where $u_{\max} \in \mathbb{R}^m$ is a vector of the maximum torques that the robot's motors are capable of producing.

However, the linear system of inequalities on μ described by both the RES-CLF convergence constraints (19) and the torque bounds (20) is not guaranteed to have a feasible solution; thus, a "relaxation" term $\delta > 0$ is added to the RES-CLF constraint:

$$L_F V_\varepsilon + L_G V_\varepsilon \mu \leq -\frac{\gamma}{\varepsilon} V_\varepsilon + \delta, \tag{21}$$

to allow V_ε to drift (locally) in the presence of active torque constraints. Using this relaxed form of the RES-CLF constraint, the torque-bounded, RES-CLF quadratic program of interest in this paper (first stated in [7], see [3] for additional related QP constructions), is given by:

$$\begin{aligned} (\mu^*, \delta^*) = \underset{(\mu,\delta)\in\mathbb{R}^{m+1}}{\operatorname{argmin}} \; & \mu^T\mu + p\delta^2 \qquad \text{(RES-CLF QP)} \\ \text{s.t.} \quad & L_F V_\varepsilon + L_G V_\varepsilon \mu \leq -\frac{\gamma}{\varepsilon} V_\varepsilon + \delta, \\ & A^{-1}(-L_f + \mu) \leq u_{\max}, \\ & -A^{-1}(-L_f + \mu) \leq u_{\max}, \end{aligned}$$

where $p > 0$ penalizes violation of the RES-CLF constraint. When there exists a μ that satisfies both the RES-CLF and the torque constraints, the solution of (RES-CLF QP) is equivalent to the min-norm controller [6]. However, when the torque constraints become active, δ^* grows and the RES-CLF constraint violated. By penalizing δ^* in the objective function, the QP finds the minimum RES-CLF violation needed to satisfy the torque bounds.

The RES-CLF QP solves for the locally optimal balance between convergence and torque bounds, however, it does not have the machinery to reason about the current globally optimal choice. As an intermediate step between the RES-CLF and re-solving the nonlinear optimization, we propose the following MPC approach.

III. MPC for Bipedal Robotic Walking

This section presents the main contribution of the paper: a model predictive control scheme which produces a current value of μ that is consistent with a finite-time forward horizon plan which minimizes estimated future values of the RES-CLF describing the walking control objectives and satisfies future values of the torque constraints. The mapping from constraints on torque to constraints on μ over the forward horizon is calculated using a process which leverages hybrid zero dynamics. The end result takes the form of a quadratic program with linear constraints.

A. Discrete-Time Representation for Horizon Planning

The continuous-time dynamical system on the outputs given in (13) can be rewritten in discrete state-space form:

$$\eta_{k+1} = \underbrace{\begin{bmatrix} 1 & \Delta T \\ 0 & 1 \end{bmatrix}}_{F_{\Delta T}} \eta_k + \underbrace{\begin{bmatrix} 0 \\ \Delta T \end{bmatrix}}_{G_{\Delta T}} \mu_k. \tag{22}$$

with discrete time-step $\Delta T > 0$. Given an initial condition, η_0, and a sequence of control inputs, $\bar{\mu} = \{\mu_0, \mu_1, \mu_2, \dots, \mu_{k-1}\}$, the value of η after k time-steps, denoted η_k, can be obtained by successively computing (22).

The corresponding value of the RES-CLF is calculated using (14):

$$V_\varepsilon(\eta_k) = \eta_k^T P_\varepsilon \eta_k. \tag{23}$$

The goal of the model-predictive control method for bipedal robotic walking is to determine a sequence of control inputs $\bar{\mu}$ that minimizes the sum of the RES-CLF computed N steps in the future while satisfying torque constraints over the same interval. The next section describes the computation of future values of the torque constraints in the context of human-inspired control.

B. Estimating Torque Constraints via Hybrid Zero Dynamics

Let $x_k = (\theta_k, \dot{\theta}_k)^T$ represent the state of the robot k time-steps in the future, and $A_k := L_g L_f y(\theta_k)$ and $L_f := L_f^2 y(\theta_k, \dot{\theta}_k)$ be the corresponding values of the Lie derivatives of (4). Using the feedback linearization control law (11), the relationship between μ and u after k time-steps, denoted μ_k and u_k respectively, is given by

$$u_k = A_k^{-1}(-L_{f,k} + \mu_k). \tag{24}$$

The goal of this section is to estimate future values of A_k and $L_{f,k}$ so that future torque bounds can be accurately predicted.

From [1], the zero dynamics coordinates corresponding to the zero dynamics surface $\mathbf{Z}_\alpha$ given in (9) are

$$z_1 = c\theta, \tag{25}$$

$$z_2 = \gamma_0(\theta)\dot{\theta}, \tag{26}$$

with $\gamma_0(\theta)$ the first row of the inertia matrix $D(\theta)$. Assuming that we have used the Human-Inspired Optimization to obtain parameters α^* corresponding to a stable periodic orbit in the hybrid system model of our robot, the dynamics of (25) and (26) along this orbit are given by:

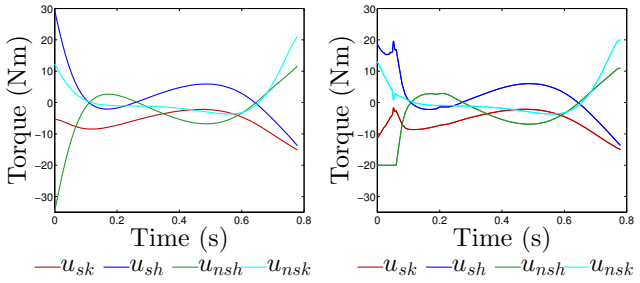

Fig. 2. Feedforward torques corresponding to the nominal gait (left) and RES-CLF QP torques with umax = 20. See [1], [4] for specific constructions of the walking outputs used in this paper.

$$\dot{z}_1 = c\Psi(z_1)z_2, \tag{27}$$

$$\dot{z}_2 = \left.\frac{\partial V(\theta)}{\partial \theta_{sf}}\right|_{\theta=\Phi(z_1)}, \tag{28}$$

where $V(\theta)$ is the potential energy of the robot and

$$\Phi(z_1) = \begin{bmatrix} c \\ H \end{bmatrix}^{-1} \begin{pmatrix} z_1 \\ y_d(z_1) \end{pmatrix}, \tag{29}$$

$$\Psi(z_1) = \begin{bmatrix} \gamma_0(\Phi(z_1)) \\ H - \frac{\partial y_d(z_1)}{\partial z_1} c \end{bmatrix}^{-1} \begin{pmatrix} 1 \\ 0 \end{pmatrix}. \tag{30}$$

It follows that on the zero dynamics surface, the angles and velocities can be calculated as functions of z_1 and z_2, $\theta = \Phi(z_1)$ and $\dot{\theta} = \Psi(z_1)z_2$. Thus, to calculate the Lie derivatives A_k and $L_{f,k}$, the zero dynamics (27) and (28) are integrated k time steps in the future to produce $z_{1,k}$ and $z_{2,k}$, which can be used to calculate angles and velocities through $\Phi(z_1)$ and $\Psi(z_1)$, which can then be used to calculate $A_k := L_g L_f y(\Phi(z_{1,k}))$ and $L_{f,k} := L_f^2 y(\Phi(z_{1,k}), \Psi(z_{1,k})z_{2,k})$.

C. MPC-QP for Bipedal Robotic Walking

We can now state the main contribution of the paper: a MPC-based quadratic program which attempts to minimize the values of the RES-CLF for robotic walking over an N time-step forward horizon and to satisfy nonlinear torque bounds over the same horizon ($R = R^T > 0$):

$$\begin{aligned} \bar{\mu}^*(x) = \underset{\bar{\mu}}{\operatorname{argmin}} \; & \eta_N^T P_\varepsilon \eta_N + \sum_{k=0}^{N-1} \eta_k^T P_\varepsilon \eta_k + \mu_k^T R \mu_k \\ \text{s.t.} \quad & \eta_{k+1} = F_{\Delta T}\eta_k + G_{\Delta T}\mu_k, \\ & A_k^{-1}\mu_k \le u^{\max} + A_k^{-1}L_{f,k}^2, \\ & -A_k^{-1}\mu_k \le u^{\max} - A_k^{-1}L_{f,k}^2, \\ & \eta_0 = \eta(x), \\ & \forall k \in \{0, 1, \dots, N-1\}. \end{aligned} \tag{31}$$

The MPC-QP is implemented in real-time. At each x, the zero dynamics coordinates are calculated using (25) and (26), and integrated forward in time to produce A_k and $L_{f,k}$. The optimization problem is then solved, and the first element in the solution, μ_0^* is used in the feedback linearization control law (11), i.e. $u = A^{-1}(-L_f + \mu_0^*)$.

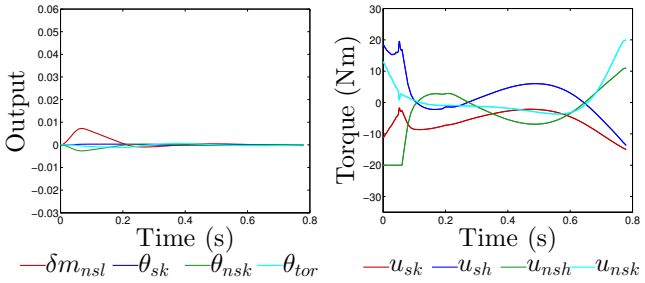

Fig. 3. Control outputs y (left) and torques u (right) from simulation using the RES-CLF QP with $u^{\max} = 20$Nm.

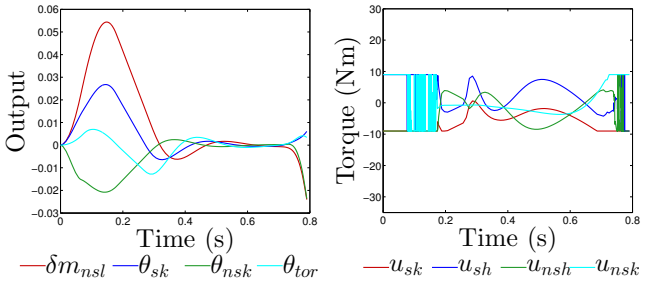

Fig. 4. Control outputs y (left) and torques u (right) from simulation using the RES-CLF QP with $u^{\max} = 9$Nm.

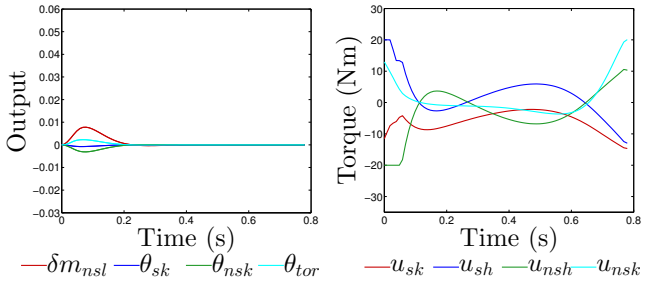

Fig. 5. Control outputs y (left) and torques u (right) from simulation using the proposed MPC-based QP with $u^{\max} = 20$Nm.

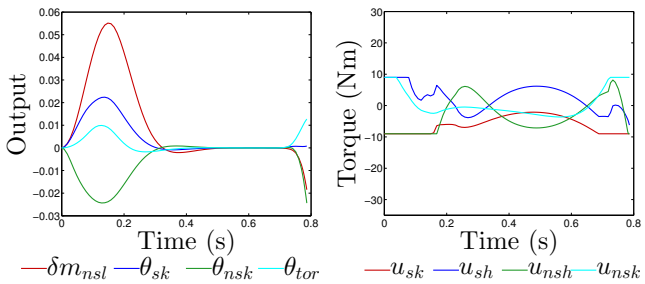

Fig. 6. Control outputs y (left) and torques u (right) from simulation using the proposed MPC-based QP with $u^{\max} = 9$Nm.

IV. Simulation Results

This section presents a simulation comparison of the performance of the RES-CLF QP [2], [7] and the proposed MPC-based control method for achieving bipedal robotic walking. The dynamic model used in this simulation is that of Durus, a robot designed and constructed by SRI International, shown in Figure 7; specifics of the model, including the coordinates, mass and length properties, can be found in [4].

As part of a different project, the Human-Inspired Optimization [1], [4] was solved to obtain parameters, α^*, and a fixed point, x^*, corresponding to a stable walking gait on a rigid-body dynamics model of the Durus robot. The desired outputs (8), computed with α^*, are shown in Figure 1, along with the periodic orbit corresponding to x^*. The nominal torques (11) along this orbit are shown in Figure 2. Here, these parameters are used to investigate the performance properties of the RES-CLF QP and the proposed MPC under non-trivial torque bounds.

A. RES-CLF QP

The first simulation case investigated is the feedback linearization controller (11) with μ obtained from (RES-CLF QP) under torque bounds of $u^{\max} = 20$Nm, $\varepsilon = 1/50$ and $p = 1$. Results from application of this controller to the robot control system (2) over the course of one continuous-time stride of walking are shown in Figure 3. The plot of the outputs y shows divergence during the initial 0.1s of simulation, and the plot of the torques u shows that one of the torques saturates during the same interval. After the initial saturation, the outputs converge as expected.

In the second simulation of the (RES-CLF QP), more rigorous torque bounds of $u^{\max} = 9$Nm are enforced, while the other configuration variables remain at $\varepsilon = 1/50$ and $p = 1$. Results from simulation of this controller are given in Figure 4. The plot of the outputs shows significantly more divergence in this case, which is to be expected given the more stringent torque bounds. The plot of the corresponding torques, however, reveals longer periods of saturation and a loss of continuity in the torque signal. This (loss of Lipschitz continuity of the commanded torques) is a recurring challenge with RES-CLF QP implementation [16].

B. MPC-QP for Bipedal Robotic Walking

The next two simulation case studies investigate the behavior of the feedback linearization controller (11) with μ obtained from the proposed MPC-based QP for bipedal robotic walking (31) described in Section III. For both simulations that follow, $N = 5$, $\Delta T = 0.01$s, $\varepsilon = 1/200$ and $R = 0.0001I$, with I an identity matrix.

In the first of the two MPC-based QP simulations, the torque bound is set to $u^{\max} = 20$Nm. Figure 5 shows outputs and torques from this simulation, in which it can be seen that (31) performs in a similar manner to (RES-CLF QP) under the same torque bounds.

In the second of the two MPC-based QP simulations, the torque bound is set to $u^{\max} = 9$Nm. Figure 6 shows outputs and torques from this simulation, in which it can be seen that the outputs y diverge in a similar manner as the outputs of the (RES-CLF QP) under the same torque bounds, but the torques produced by the IO-MPC do not lose Lipschitz continuity.

V. Experimental Results and Future Work

The proposed MPC-based controller for bipedal robotic walking was implemented in C++ on the Durus robot using an internal dynamics model integration method to convert the feedback linearization torques into position and velocity commands [4]. Data from an experiment in which the robot successfully completed three laps around the room (63 steps) is shown in Figure 7. The average phase portraits from experiment agree quite well with the corresponding phase portraits from simulation, presented earlier in Figure 1. In the experiment phase portrait, bi-periodicity is apparent: this is due to the fact that the boom which supports Durus does not entirely enforce planar motion. A video of the experiment is available online `http://youtu.be/OG-WIfWMZek`.

Formal stability of the hybrid periodic orbit as a result of the proposed MPC control approach is a prime focus of current research. Existing methods of proving stability of the orbit rely on exponential stability of the continuous-time controller, and to the authors' knowledge, a proof of stability under nontrivial torque saturation is still an open problem. To address the hybrid stability problem, it will be important to note existing methods of proving stability of MPC controllers, such as those described in [14], impose conditions on a terminal cost $\eta_N^T P_\varepsilon \eta_N$. *Zero dynamics* play a large part in the current work. Increasing the dimensionality of the zero dynamics (such as going to 3D) poses significant challenges that need to be addressed. *A note on the method:* the proposed MPC problem is (currently) not intended to replace the nonlinear optimization that produces the nominal gait. Associated with the nominal gait is a feedforward torque profile; deviations from these nominal torques will necessarily change the gait. The standard approach would be to re-solve the constrained nonlinear optimization for a different gait with lower torque bounds; however, this comes with its own challenges and it has to be done offline. Instead, the current MPC formulation intends to be a step towards handling (reasonable) torque bounds at the online control implementation level, and thus, relieve some of the burden of the offline optimization.

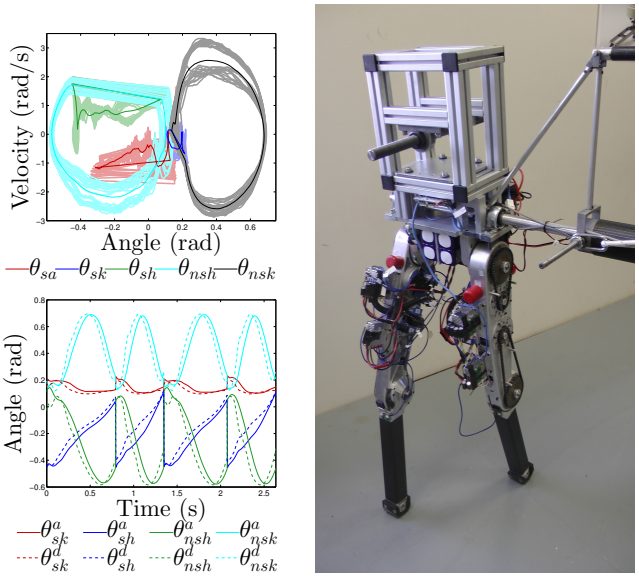

Fig. 7. Results from experiment of the proposed MPC-based QP for robotic walking with Durus (right), showing phase portraits (top left) for 63 steps of walking together with a darker averaged phase portrait and position tracking errors (bottom left) over a select 4 steps in the same experiment.

References

[1] A. D. Ames. Human-inspired control of bipedal walking robots. *Automatic Control, IEEE Transactions on*, 2014.

[2] A. D. Ames, K. Galloway, and J. W. Grizzle. Control lyapunov functions and hybrid zero dynamics. In *Decision and Control (CDC), 2012 IEEE 51st Annual Conference on*, 2012.

[3] A. D. Ames and M. Powell. Towards the unification of locomotion and manipulation through control lyapunov functions and quadratic programs. In *Control of Cyber-Physical Systems*, Lecture Notes in Control and Information Sciences. 2013.

[4] E. Cousineau and A. D. Ames. Realizing underactuated bipedal walking with torque controllers via the ideal model resolved motion method. *IEEE International Conference on Robotics and Automation (ICRA)*, 2015.

[5] J. Deng, V. Becerra, and R. Stobart. Input constraints handling in an mpc/feedback linearization scheme. *Int. J. Appl. Math. Comput. Sci.*, 2009.

[6] R. A. Freeman and P. V. Kokotović. *Robust Nonlinear Control Design*. Birkhäuser, 1996.

[7] K. S. Galloway, K. Sreenath, A. D. Ames, and J. W. Grizzle. Torque saturation in bipedal robotic walking through control lyapunov function based quadratic programs. *CoRR*, abs/1302.7314, 2013.

[8] G. Garofalo, C. Ott, and A. Albu-Schaffer. Walking control of fully actuated robots based on the bipedal slip model. In *Robotics and Automation (ICRA), 2012 IEEE International Conference on*, 2012.

[9] J. W. Grizzle and E. R. Westervelt. Hybrid zero dynamics of planar bipedal walking. In *Analysis and Design of Nonlinear Control Systems*. 2008.

[10] S. Kajita, F. Kanehiro, K. Kaneko, K. Fujiwara, K. Harada, K. Yokoi, and H. Hirukawa. Biped walking pattern generation by using preview control of zero-moment point. In *Robotics and Automation, 2003. Proceedings. ICRA '03. IEEE International Conference on*, 2003.

[11] X.-B. Kong, Y. jie Chen, and X. jie Liu. Nonlinear model predictive control with input-output linearization. In *Control and Decision Conference (CCDC), 2012 24th Chinese*, 2012.

[12] S. Kuindersma, F. Permenter, and R. Tedrake. An efficiently solvable quadratic program for stabilizing dynamic locomotion. *CoRR*, 2013.

[13] M. J. Kurtz and M. A. Henson. Input-output linearizing control of constrained nonlinear processes. *Journal of Process Control*, 1997.

[14] D. Q. Mayne, J. B. Rawlings, C. V. Rao, and P. O. M. Scokaert. Survey constrained model predictive control: Stability and optimality. *Automatica*, 2000.

[15] B. Morris and J. Grizzle. A restricted poincar'e; map for determining exponentially stable periodic orbits in systems with impulse effects: Application to bipedal robots. In *Decision and Control, CDC-ECC. 44th IEEE Conference on*, 2005.

[16] B. Morris, M. Powell, and A. Ames. Sufficient conditions for the lipschitz continuity of qp-based multi-objective control of humanoid robots. In *IEEE Conference on Decision and Control (CDC)*, 2013.

[17] R. M. Murray, Z. Li, and S. S. Sastry. *A Mathematical Introduction to Robotic Manipulation*. CRC Press, Boca Raton, 1994.

[18] M. Posa and R. Tedrake. Direct trajectory optimization of rigid body dynamical systems through contact. In *Algorithmic Foundations of Robotics X*, Springer Tracts in Advanced Robotics. 2013.

[19] J. Pratt, J. Carff, and S. Drakunov. Capture point: A step toward humanoid push recovery. In *6th IEEE-RAS International Conference on Humanoid Robots*, Genoa, Italy, 2006.

[20] S. S. Sastry. *Nonlinear Systems: Analysis, Stability and Control*. Springer, New York, 1999.

[21] M. W. Spong and M. Vidyasagar. *Robotic Dynamics and Control*. John Wiley and Sons, New York, NY, 1989.

[22] B. Stephens and C. Atkeson. Push recovery by stepping for humanoid robots with force controlled joints. In *International Conference on Humanoid Robots*, Nashville, Tennessee, 2010.